STRUCTURAL APPLICATIONS OF FERRITIC STAINLESS STEELS (SAFSS)

Report To: RFCS
Document: Characterization of Stress–Strain Behavior
Version: 01
Date: May 2013

Version	Date of Issue	Purpose	Author	Technical Reviewer	Approved
01	30.5.2013	Issue to RFCS and TGS8	TPM	JSk	MYI

The testing, assessment, findings and conclusions outlined in this report have been made with the intent of due diligence, care and best effort. Despite that we may not be held liable for any direct, compensatory or consequential loss or damage exceeding the amount paid for this report.

EUROPEAN COMMISSION

Research Programme of
The Research Fund for Coal and Steel - Steel RTD

Title of Research Project:	**Structural Application of Ferritic Stainless Steels (SAFSS)**
Executive Committee:	**TGS8**
Contract:	**RFSR-CT-2010-00026**
Commencement Date:	**July 01, 2010**
Completion Date:	**May 30, 2013**
Work Package No and Title:	**WP1, End-user Requirements and Material Performance**
Final Report:	**WP1.3, Characterization of Stress–Strain Behavior**
Beneficiary:	**Outokumpu Stainless Oy** **95490 Tornio, Finland**
Research Location:	**Outokumpu Stainless Oy** **Tornio Research Centre** **95490 Tornio, Finland**
Contact person:	**Jukka Säynäjäkangas**
Report authors:	**Timo Manninen**

Summary

The present report summarizes the test results obtained from the tension and compression testing of commercial ferritic stainless steels. The objective of this work was to determine the relevant basic mechanical property data, which designers need in order to design the targeted structural applications.

Ferritic stainless steels have different mechanical properties from carbon steels and other families of stainless steels. In general, ferritic stainless steel grades have higher yield strength and lower ductility than austenitic ones.

Laboratory tests were carried out to measure the stress-strain characteristics of commercial ferritic stainless steels. This information is needed for predicting the behaviour of load bearing structural members under different loading conditions. The grades 1.4003, 1.4016, 1.4509, 1.4521 and 1.4621 were studied in this work. The material properties were determined for virgin sheets supplied by three European steel producers. Uniaxial tension and compression tests were carried out on samples orientated in the longitudinal and transverse directions. The compression testing was carried out using adhesively bonded specimens.

The test results contain information on the strength, ductility and stiffness characteristics of commercial ferritic stainless steels. In addition, characteristic values were determined for the coefficient *n* defining the non-linearity of the stress-strain curve. The data generated contains suitable guidance to be included in the Eurocode EN 1993-1-4.

Contents

1 Introduction

Ferritic stainless steels are low cost, price-stable, corrosion-resistant steels. In contrast to austenitic grades, ferritic stainless steels are ferromagnetic, they have low thermal expansion and high thermal conductivity, and they are immune for chloride-induced stress-corrosion cracking.

Ferritics are widely used in the automotive and household appliance sectors. Structural applications of these materials in the construction industry are, however, scarce. One major barrier to the wider use of ferritic stainless steels in construction is the lack of relevant design guidance.

The RFCS funded project Structural Applications for Ferritic Stainless Steels aims to generate efficient and economical design guidance for optimal use of ferritic stainless steels in the construction industry.

Ferritic stainless steels have different mechanical properties from carbon steels and other families of stainless steels. In general, the ferritic stainless steel grades have higher yield strength and lower ductility than the austenitic ones.

The present report summarizes the test results obtained from the tension and compression testing of commercial ferritic stainless steels. The objective of this work was to determine the basic mechanical property data needed for structural design purposes. The grades 1.4003, 1.4016, 1.4509, 1.4521 and 1.4621 were studied. The material properties were determined for hot-rolled and cold-rolled virgin sheets supplied by three European stainless steel producers AcerInox, Aperam and Outokumpu. Uniaxial tension and compression tests were carried out on samples orientated in the longitudinal and transverse directions. The compression testing was carried out using adhesively bonded specimens.

The data generated contain information on the strength, ductility and stiffness characteristics of commercial ferritic stainless steels. In addition, characteristic values were determined for the coefficient *n* defining the non-linearity of the stress-strain curve. The data generated contains suitable guidance to be included in the Eurocode EN 1993-1-4.

2 Objectives

The objective of this task was to determine the basic information on the stress-strain behaviour of ferritic stainless steels needed for developing Eurocode-aligned structural design guidance for these steels. The emphasis was on grades included the in newly issued material specification EN 10088-4 which have not been studied before.

Uniaxial tension and compression tests were carried out on samples orientated in the longitudinal and transverse directions in order to generate the relevant mechanical property data on the strength, ductility and stiffness characteristics of studied steels. The relevant data includes the characteristic values for the coefficient *n* defining the non-linearity of the stress-strain curve.

3 Experimental work

3.1 Test materials

In total 10 materials from three suppliers were studied. Two of the materials were in hot-rolled and eight in cold-rolled condition. The materials and their chemical compositions are given in Table 1. The material properties were determined for virgin sheets. Material from two suppliers was studied for the grades 1.4016, 1.4509 and 1.4521. The grade 1.4621 was only available from one supplier. The grade 1.4003, which has been extensively studied in earlier ESCS/RFCS funded projects, was included as a reference material.

Table 1. Chemical composition of test materials (wt-%).

Sample	Grade	Supplier	Type	Thickness	C	Si	Mn	Cr	Ni	Mo	Ti	Nb	Cu	Al	N	KFF
4003-1	1.4003	B	CR	2.0	0.015	0.26	1.45	11.4	0.4	0.0	0.00	0.01	0.1	0.00	0.013	7.4
4016-1	1.4016	C	CR	2.0	0.023	0.36	0.46	16.3	0.2	0.0	0.01	0.01	0.1	0.01	0.028	14.8
4016-2	1.4016	B	CR	2.0	0.046	0.30	0.48	16.1	0.2	0.2	0.00	0.02	0.1	0.00	0.027	14.1
4016-3	1.4016	C	HR	3.0	0.064	0.27	0.32	16.1	0.1	0.0	0.01	0.01	0.1	0.01	0.025	13.2
4509-1	1.4509	C	CR	2.0	0.017	0.55	0.45	17.8	0.2	0.0	0.14	0.49	0.0	0.05	0.018	19.3
4509-2	1.4509	B	CR	2.0	0.020	0.55	0.48	17.9	0.3	0.0	0.12	0.40	0.1	0.01	0.030	18.4
4509-3	1.4509	C	HR	3.5	0.018	0.36	0.26	17.6	0.2	0.0	0.16	0.47	0.1	0.07	0.019	18.4
4521-1	1.4521	C	CR	2.0	0.011	0.48	0.44	17.7	0.3	2.0	0.17	0.43	0.1	0.00	0.016	26.6
4521-2	1.4521	B	CR	2.0	0.015	0.52	0.49	18.0	0.1	2.0	0.13	0.40	0.2	0.01	0.019	27.3
4621-1	1.4621	A	CR	1.5	0.014	0.21	0.23	20.6	0.2	0.0	0.01	0.45	0.4	0.00	0.014	19.7

CR = cold-rolled strip, HR = hot-rolled strip, KFF = Kaltenhauser ferrite factor

3.2 Test procedures

The room temperature tensile and compression testing is performed by means of a Zwick Z250/SW5A tensile testing machine with the capacity of 250kN, Figure 1. The tensile testing machine is equipped with GTM load cell no. 30971, hydraulic specimen grips and Zwick B06650 macro extensometer, Figure 2. The clamping of the sensor arms and the setting of the original gauge length L_0 is automatic with this extensometer type. The equipment is regularly calibrated according to standards SFS-EN ISO 7500-1:2004 and SFS-EN ISO 9513:2002.

Figure 1. The Zwick / Roell Z250 tensile test machine.

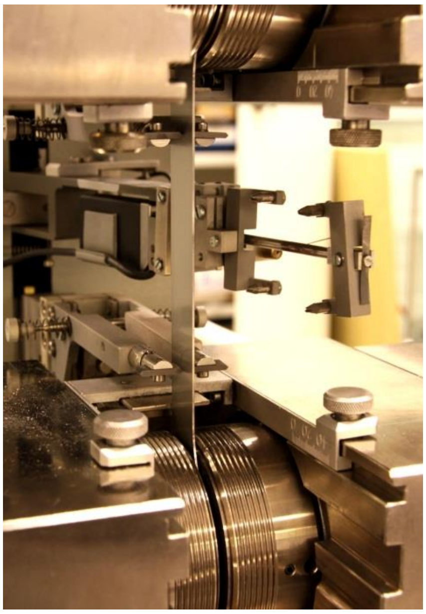

Figure 2. Hydraulic grips and Zwick Macro extensometer with motorized sensor arms.

3.2.1. Test piece used for compression testing

In-plane compression testing of sheet metals was performed by employing adhesively bonded laminated specimens. The laminated test pieces were obtained in two steps. First rectangular preforms of size 25 x 235 mm were adhesively bonded into a laminated stack of thickness greater than 15 mm. After the adhesive had cured, the test piece was machined from the laminated stack.

The adhesive used was the two-component epoxy-based adhesive Loctite Hysol 9466. The shear strength of the adhesive, measured according to ISO 4587, is 37 MPa. Due to the high strength of the adhesive, de-bonding occurs only after the buckling of the specimen. The thickness of each adhesive layer was roughly 0.2 mm. Consequently, the influence of the adhesive on the stress-strain curve is negligible. Before applying the adhesive, the bonding surfaces were lightly ground with 60-grit sandpaper and the surfaces were cleaned with acetone to dissolve oils and fats. After applying the adhesive on the surfaces, the stack was compressed with a hand press and allowed to cure for 24 hours.

The test piece geometry is shown in Figure 3 and Figure 4.The geometry is adapted from the tensile test specimen of type 1 in annex B of EN ISO 6892-1 by reducing the parallel length to 35mm. The original gauge length used in the compressive testing is $L_0 = 25mm$.

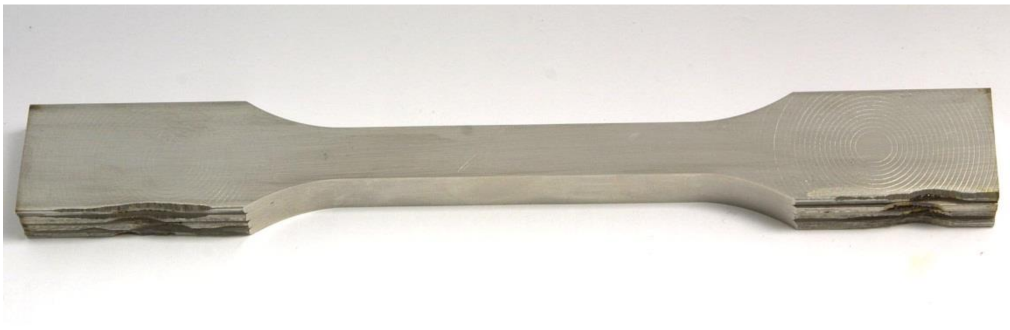

Figure 3. Laminated test piece used for compression testing.

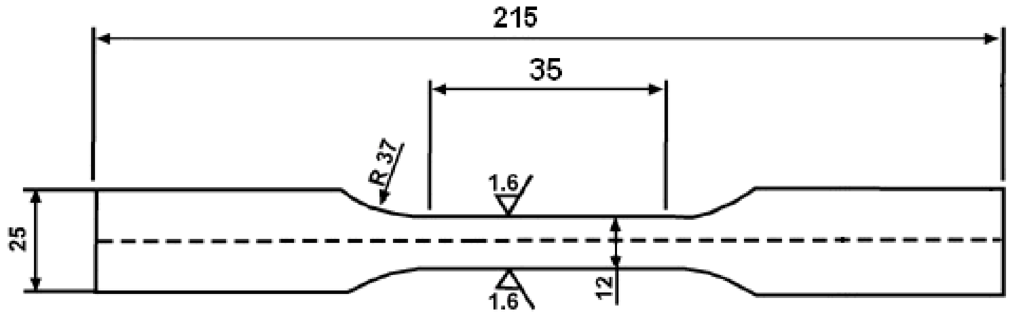

Figure 4. Geometry of the test piece used for compression testing.

3.2.2. Validation of the compression test specimen against buckling

A validation test series was carried out using Outokumpu 1.4003 and 1.4509 with the thickness of 2mm to verify that premature buckling or delamination does not occur in the test before the target compressive strain of 2% is reached. Strain gages were attached to the neighbouring faces of the specimen to monitor the strain on the outer surfaces of the specimen. By comparing the compressive the signals of the strain gages, the onset of bucking could be detected. The results showed that the present test setup is capable of reaching the target strains of 2% before the onset of buckling or delamination. The typical strain for the onset of bucking or delamination in the validation tests was approximately 6%, i.e. three times the target strain.

3.2.3. Specimens for tension testing

Two different test piece types were used depending on the material thickness. The test pieces were obtained by machining or by laser cutting. The results of a comprehensive testing program carried out at Outokumpu Tornio Research Centre have shown that the laser cutting does not have an influence on the test results for materials thinner than 6 mm. The test piece geometry for materials with thickness less than 3 mm is shown in Figure 5. This test piece geometry corresponds to test piece type 2 in the Annex B of SFS-EN ISO 6892-1. The original gauge length used for the test piece is $L_0 = 80mm$.

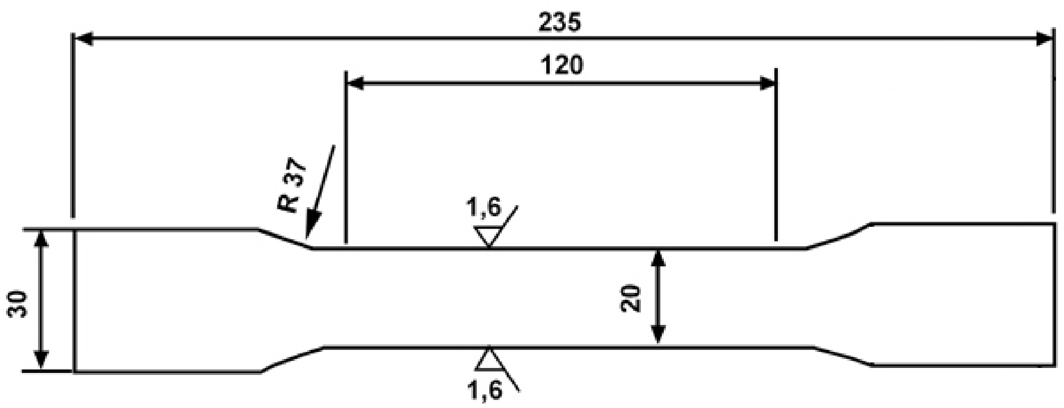

Figure 5. The tension test piece geometry for materials with thickness less than 3mm.

The test piece geometry for sheets with thickness equal or more than 3mm is shown in Figure 6. This test piece geometry corresponds to type 1 in the annex B of EN ISO 6892-1. The original gauge length used for this test piece type is $L_0 = 50mm$.

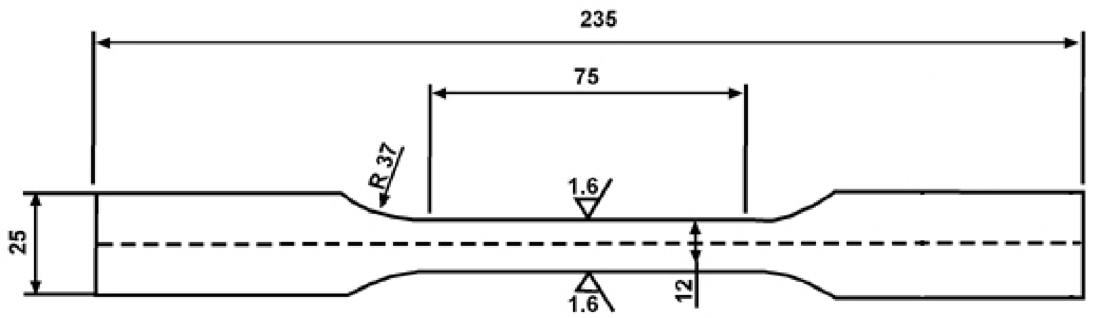

Figure 6. The tension test piece geometry for materials with thickness ≥ 3mm.

3.2.4. Conditions of testing for compression testing

The compression testing was performed, as much as possible, by following the tensile test standard SFS-EN 10002-1. The crosshead speed of 0.8 mm/min was used throughout the test. This crosshead speed results in the straining rate value of 0.00025 s^{-1}. The same straining rate was used in the initial parts of tensile testing as described in the next chapter. The compression tests were continued until the specimen failed by buckling or by deponding or until the maximum compressive strain of 2% was reached.

3.2.5. Conditions of testing for tension testing

The tensile testing was performed according to the tensile test standard EN ISO 6892-1. The tensile testing standard specifies two different methods of controlling the machine rate in different parts of the tensile testing. The method A224 for strain rate based machine control was used in the testing program. The relevant strain rate values are given in Table 2.

A validation test series was carried out using Outokumpu 1.4003, 1.4509 and 1.4521 with the thickness of 2 mm to verify that loading rate conforms to the requirements of the standard. The results showed that the straining rate was within the specified limits. An example stress-strain curve measured in the validation test series is shown in Figure 7. The straining rate, calculated from the measured data, is shown in Figure 8. It can be seen that the straining rate is very accurately constant and within the specified tolerances.

It is worth noting that the sudden change of testing speed at the nominal strain of 2.5% results in a sharp step in the stress strain curve. The step is also clearly visible in the example curve in Figure 8. The size of the step depended only on the steel grade; it was independent on the supplier and on delivery condition. For the unstabilized grades 1.4003 and 1.4016, the size of the step was approximately 12 MPa. For the stabilized grades 1.4509, 1.4521 and 1.4621, the size of the step was approximately 16 MPa.

Table 2. Loading rates in the EN ISO 6892-1:2009 method A224.

Range	Straining rate (s^{-1})	Relative tolerance
Elastic range	0,00025	± 20%
Proof stress	0,00025	± 20%
Tensile strength	0,0067	± 20%

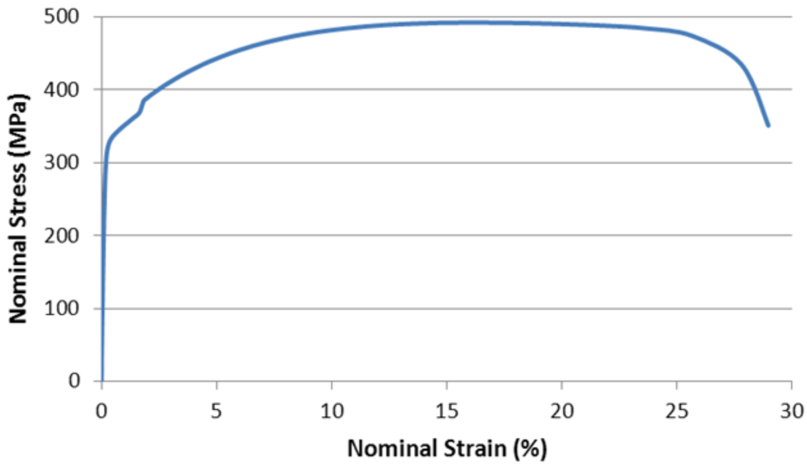

Figure 7. Stress-strain curve measured for 2mm Outokumpu 1.4003 in a validation test.

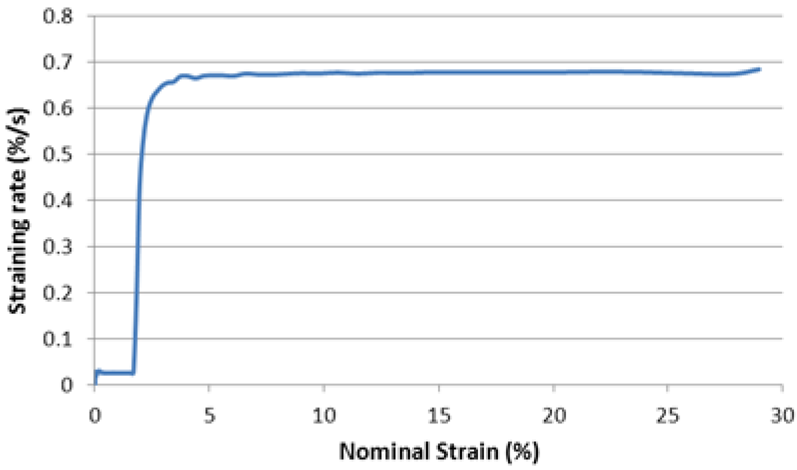

Figure 8. The straining rate for 2mm Outokumpu 1.4003 in the validation test.

4 Results and observations

This section contains the results of tension and compression tests. Only the essential information is given. The full results including the obtained stress-strain curves are included in the appendices.

4.1 Results of tension testing

4.1.1 Strength and ductility

The room temperature tensile test results are summarized in Table 3. The values given in the table are average values for three repeats. Discontinuous yielding in the form of an upper and lower yield point or yield point elongation was not observed in the tests.

Table 3. Tension test results for all test materials.

Steel	Direction	Type	E-Modulus	Rp0,01	Rp0,1	Rp0,2	Rp1,0	Rm	Ag	A*	A5
			GPa	N/mm²	N/mm²	N/mm²	N/mm²	N/mm²	%	%	%
4003-1	RD	CR	194	234	318	330	357	493	16.2	31	51
4003-1	TD	CR	202	282	347	357	378	497	16.0	29	46
4016-1	RD	CR	190	225	299	311	338	478	16.8	26	38
4016-1	TD	CR	218	277	336	344	366	496	16.0	28	42
4016-2	RD	CR	175	237	305	315	333	458	17.4	33	53
4016-2	TD	CR	201	304	345	349	364	482	15.6	32	51
4016-3	RD	HR	199	235	322	338	367	475	12.9	21	25
4016-3	TD	HR	222	295	364	379	408	524	12.0	(15)	(16)
4509-1	RD	CR	201	250	321	331	353	479	17.6	29	43
4509-1	TD	CR	221	289	344	351	369	489	16.4	29	44
4509-2	RD	CR	195	287	358	367	384	488	15.9	33	54
4509-2	TD	CR	207	337	382	389	403	497	14.9	33	56
4509-3	RD	HR	204	321	420	440	462	524	9.7	21	25
4509-3	TD	HR	231	427	502	513	524	579	8.1	20	24
4521-1	RD	CR	192	291	367	375	396	542	16.2	29	45
4521-1	TD	CR	210	357	399	401	418	559	15.3	28	43
4521-2	RD	CR	195	309	382	394	419	564	15.6	28	44
4521-2	TD	CR	212	356	410	418	439	576	14.8	28	45
4621-1	RD	CR	184	279	351	359	373	469	15.9	32	56
4621-1	TD	CR	205	333	382	386	396	481	14.6	30	54

* = A80 for cold-rolled and A50 for hot-rolled strip.
( ) = Fracture occurred near the specimen shoulder, ultimate tensile strain could not be determined accurately.

The minimum strength and ductility requirements specified by the material standard prEN 10088-2:2005 are given in Table 4. A comparison of measured 0.2% proof strength values with the minimum values shows that all studied materials had considerable overstrength. On the average, the overstrength was approximately 40% of the minimum value specified by the standard, Table 5. The material standard prEN 10088-2:2005 does not specify mechanical properties for hot-rolled 1.4509. Therefore, the mechanical properties given for cold-rolled 1.4509 are used for comparison purposes in the present report. A comparison of measured elongation at fracture values with the minimum values specified by the material standard shows that all studied materials had considerable additional ductility compared to the minimum values required by the material standard. On the average, the measured elongation at fracture exceeds the corresponding requirement approximately by 50%.

Table 4. Mechanical properties at room temperature according to prEN 10088-2:2005.

Steel grade	Condition	Rp0.2 min (MPa) long.	Rp0.2 min (MPa) trans.	Tensile strength (MPa)	Elongation at fracture, min (%)
1.4003	CR	280	300	450 to 650	20
	HR	280	300	450 to 650	20
1.4016	CR	260	280	430 to 600	20
	HR	240	260	430 to 600	18
1.4521	CR	300	320	420 to 640	20
	HR	280	300	400 to 600	20
1.4509	CR	230	250	430 to 530	18
	HR	n/a	n/a	n/a	n/a
1.4621	CR	230	250	400 to 600	22
	HR	230	250	400 to 600	22

n/a = not specified in the material standard.

Table 5. Overstrength of test materials.

Steel	Average Overstrength TD	Average Overstrength RD
4003-1	19 %	18 %
4016-1	23 %	19 %
4016-2	25 %	21 %
4016-3	46 %	41 %
4509-1	40 %	44 %
4509-2	55 %	60 %
4509-3	105 %	91 %
4521-1	25 %	25 %
4521-2	31 %	31 %
4621-1	54 %	56 %
Mean	42 %	41 %
Std.dev.	26%	23%

4.1.2 Ductility and work hardening capacity

According to EN 1993-1.1, section 3.2.2, certain ductility is required of steels used for structural applications. The ductility requirements are summarized in Table 6.

Table 6. Ductility requirements for structural steel.

Property	Criterion
Work-hardening capacity	(Rm / Rp0.2) ≥ 1.10
Elongation at failure	A5 ≥ 15%
Ultimate strain	Ag ≥ 15 · (Rp0.2 / E)

All studied ferritic stainless steel grades showed considerable work hardening capacity and ductility in room temperature tension testing. Tensile test results given in Table 7 show that all studied steels conform to the minimum ductility requirements specified in the Eurocode EN 1993-1-1 and 1993-1-4. The values given are averages for three repeats. Therefore, it can be concluded that the studied steels exhibit sufficient ductility and work hardening capacity required by EN 1993-1.1 of structural steels.

Table 7. Measured ductility properties for all studied steels.

Steel	Direction	(Rm / Rp0.2)	A5	Ag	15 · (Rp0.2 / E)
		(-)	(%)	(%)	(%)
4003-1	TD	1.39	46	16.0	2.7
4003-1	RD	1.49	51	16.2	2.7
4016-1	TD	1.44	42	16.0	2.4
4016-1	RD	1.54	38	16.8	2.5
4016-2	TD	1.38	51	15.6	2.7
4016-2	RD	1.45	53	17.4	2.8
4016-3	TD	1.38	16	12.0	2.7
4016-3	RD	1.40	25	12.9	2.6
4509-1	TD	1.39	44	16.4	2.4
4509-1	RD	1.45	43	17.6	2.5
4509-2	TD	1.28	56	14.9	2.8
4509-2	RD	1.33	54	15.9	2.8
4509-3	TD	1.13	24	8.1	3.4
4509-3	RD	1.19	25	9.7	3.4
4521-1	TD	1.39	43	15.3	2.9
4521-1	RD	1.44	45	16.2	3.0
4521-2	TD	1.38	45	14.8	3.0
4521-2	RD	1.43	44	15.6	3.0
4621-1	TD	1.25	54	14.6	2.9
4621-1	RD	1.31	56	15.9	3.0

4.1.3 Anisotropy between the longitudinal and transverse yield strength values

According to the tension test results summarized in Table 3, the strength of the studied materials was typically higher in the transverse direction than in the longitudinal direction. On the average, the 0.2% proof strength was 9% higher in the transverse direction than in the longitudinal direction, Figure 9.

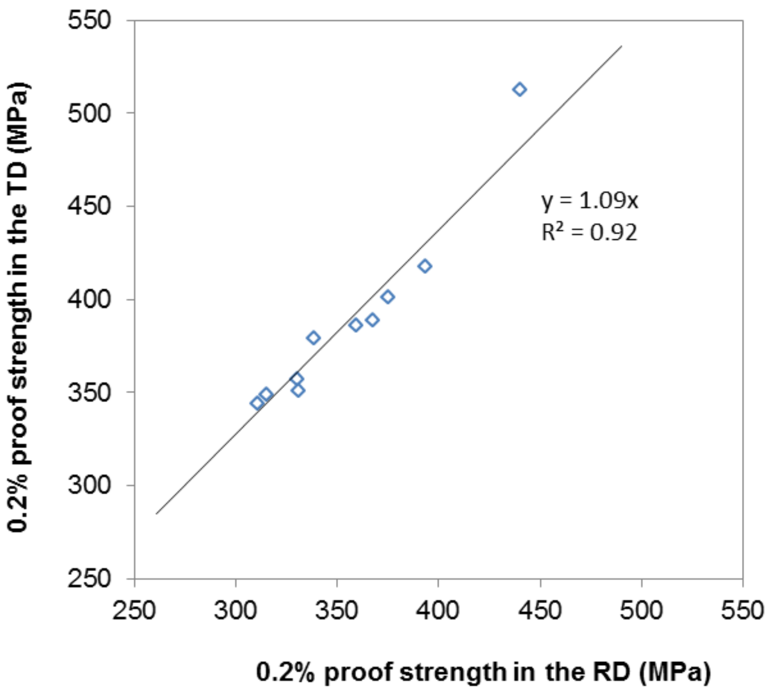

Figure 9. The correlation between 0.2% proof strength values measured in the transverse (TD) and longitudinal (RD) directions.

The experimental uncertainly of the 0.2% proof strength values can be estimated based on values given in the tensile testing standard ISO EN 6892-1:2009 for austenitic stainless steels. Based on the values given in the testing standard, the expanded experimental uncertainty of 0.2% proof strength was estimated to be 7.3%.

Figure 10 shows the 0.2% proof stress values along with the upper and lower limit curves corresponding to the 7.3% uncertainty due to material scatter and measurement uncertainty. It can be seen that the difference between the proof strength values does not fall within the typical experimental scatter in the 0.2% proof stress values. Therefore, the difference is statistically significant.

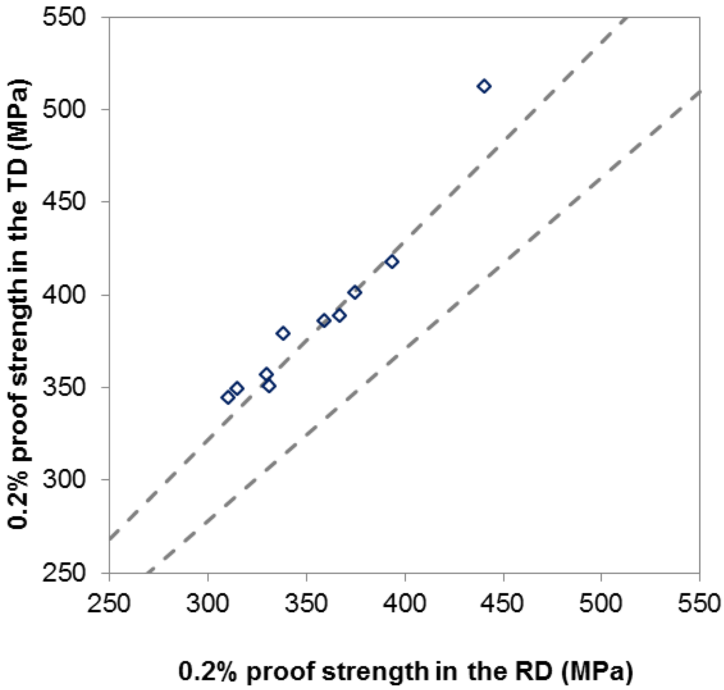

Figure 10. The 0.2% proof strength values measured in the transverse (TD) and longitudinal (RD) directions along with the upper and lower bounds corresponding to the experimental uncertainty of 0.2% proof strength in tension testing.

4.2 Results of compression testing

Compression test were carried out on all test material using laminated dog-bone shaped test pieces as described in the chapter 3.2 above. The compression test results are summarized in Table 8. The values given in the table are average values for three repeats.

A comparison of proof strength values measured in tension and in compression shows that the tension-compression asymmetry was small for all studied steels. Figure 12 shows the 0.2% proof stress values measured in compression against the corresponding values measured in tension for all studied steels. Upper and lower limit curves corresponding to the 7.3% experimental uncertainty are shown for reference. It can be concluded that the difference between tensile and compressive proof strength values is smaller than the experimental uncertainty. Therefore, the difference is not significant.

The repeatability was generally good in compression tests. Figure 11 shows an example. One stress-strain curve measured in tension is shown for reference. The curves are presented in the true stress and true strain coordinates in order to account for the different change of cross-sectional area in the two test methods. There is a negligible difference between the stress-strain behaviour measured in uniaxial tension and that measured in uniaxial compression.

Table 8. Compression test results for all test materials.

Steel	Direction	Type	E-Modulus	Rp0,01	Rp0,1	Rp0,2	Rp1,0
			GPa	N/mm²	N/mm²	N/mm²	N/mm²
4003-1	RD	CR	205	206	290	310	357
4003-1	TD	CR	232	279	351	362	391
4016-1	RD	CR	184	201	281	300	342
4016-1	TD	CR	218	267	332	343	379
4016-2	RD	CR	186	214	294	311	345
4016-2	TD	CR	215	266	342	351	376
4016-3	RD	HR	206	218	317	334	371
4016-3	TD	HR	232	297	386	398	431
4509-1	RD	CR	206	193	298	322	361
4509-1	TD	CR	217	261	340	352	381
4509-2	RD	CR	207	234	342	361	397
4509-2	TD	CR	222	300	379	389	415
4509-3	RD	HR	212	269	413	442	481
4509-3	TD	HR	239	356	492	510	535
4521-1	RD	CR	214	242	366	386	419
4521-1	TD	CR	297	262	396	408	433
4521-2	RD	CR	217	241	354	375	415
4521-2	TD	CR	238	333	417	429	462
4621-1	RD	CR	202	235	333	348	374
4621-1	TD	CR	277	266	370	381	399

Also in the compression testing, the proof strength values measured in the transverse direction were typically higher than the ones measured in the longitudinal direction. On the average, the 0.2% proof strength was 12% higher in the transverse direction than in the longitudinal direction, Figure 13. Figure 14 shows the 0.2% proof stress values measured in the transverse direction against the corresponding values measured in the longitudinal direction for all studied steels both in tension and in compression. Upper and lower limit curves corresponding to material scatter and measurement uncertainty are shown for reference. It can be seen that the transverse-longitudinal anisotropy is similar in tension and in compression. It is also evident that the anisotropy is significant in comparison with the experimental uncertainty.

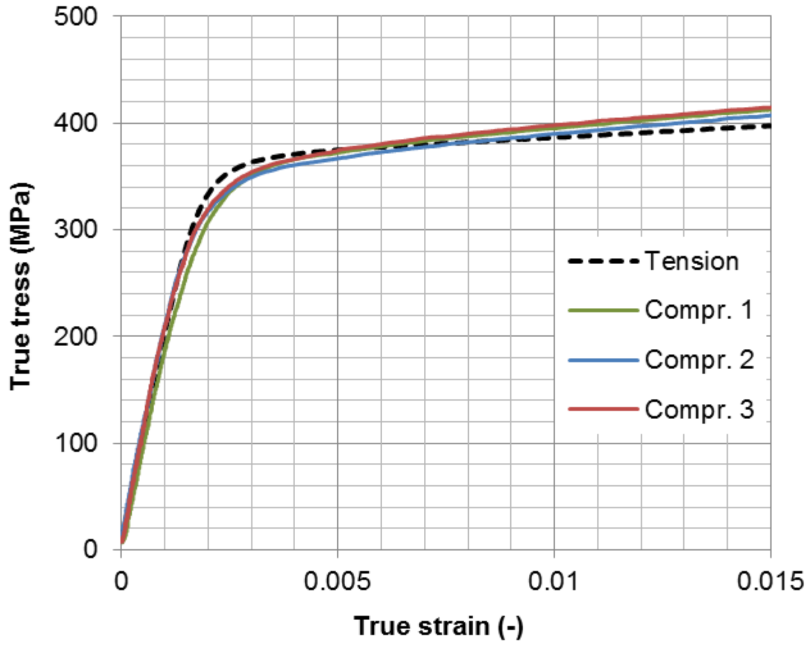

Figure 11. Compression test results for 4509-2 in the longitudinal direction. One stress-strain curve measured in tension is shown for comparison.

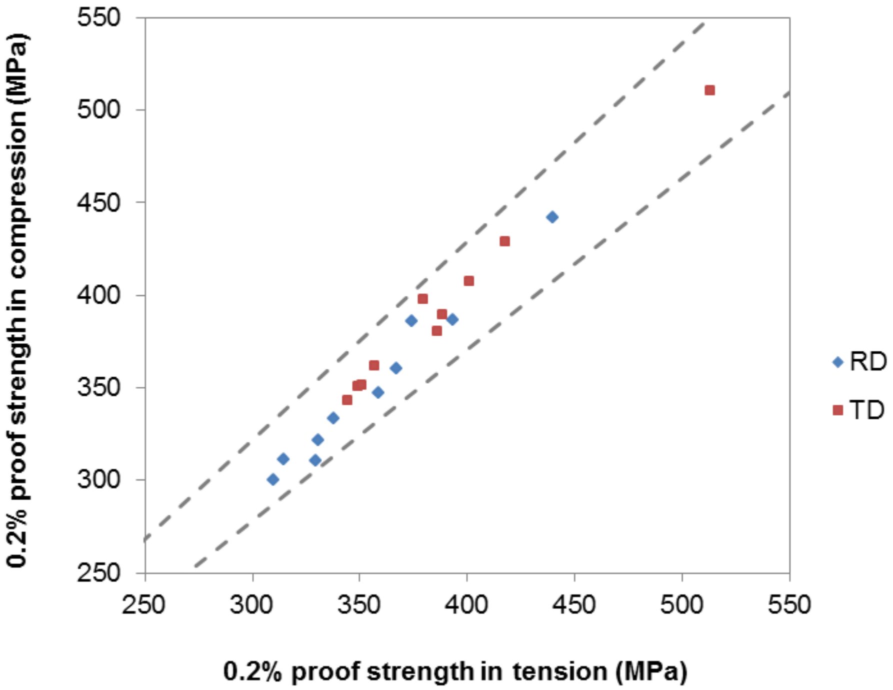

Figure 12. Correlation between the 0.2% proof strength values in tension and in compression. Upper and lower limit curves corresponding to material scatter and measurement uncertainty are shown for reference

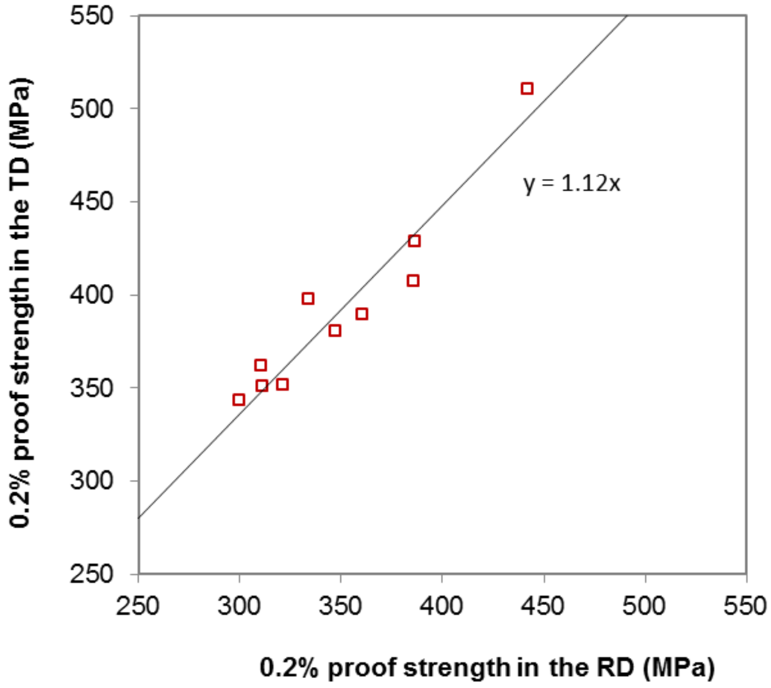

Figure 13. Correlation between the 0.2% proof strength values measured in the transverse (TD) and longitudinal (RD) directions in compression.

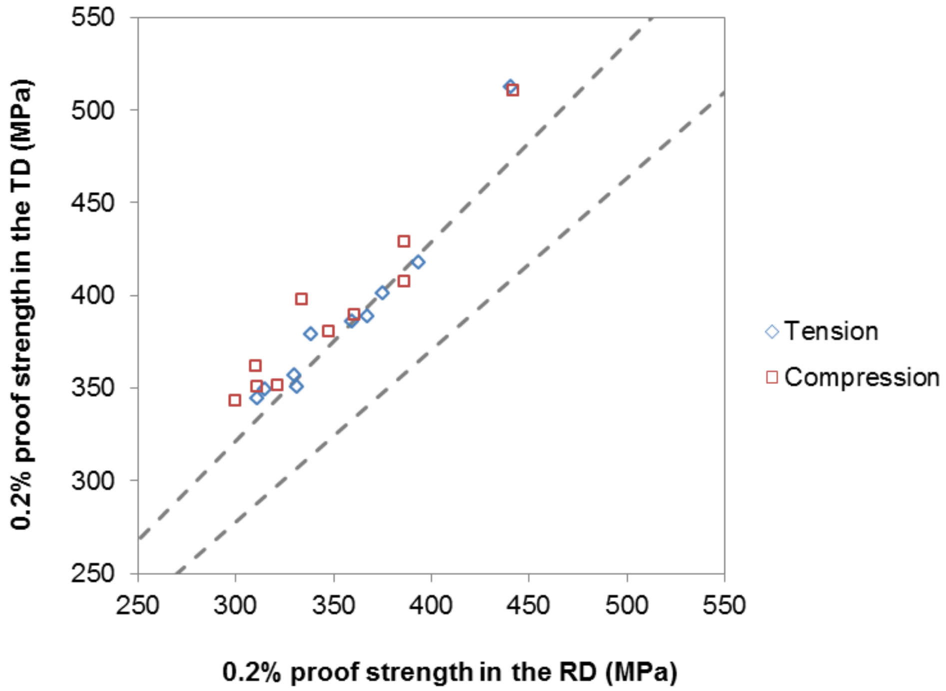

Figure 14. Correlation between the 0.2% proof strength values measured in the RD and in the TD. Upper and lower limit curves corresponding to material scatter and measurement uncertainty are shown for reference.

5 Determination of n-values

The studied ferritic stainless steels exhibit a non-linear stress–strain relationship. For design purposes, the observed stress–strain behaviour needs to be described using the Ramberg–Osgood model

$$\varepsilon = \frac{\sigma}{E_0} + 0.002 \left(\frac{\sigma}{\sigma_{0,2}}\right)^n \quad , \qquad (1)$$

where E_0 is the initial elastic modulus, $\sigma_{0.2}$ is the 0.2% proof stress and n is a material parameter. The parameter n is conventionally determined using the relation

$$n = \frac{\ln 20}{\ln\left(\frac{\sigma_{0.2}}{\sigma_{0.01}}\right)} \, . \qquad (2)$$

Recently, it has been demonstrated by Real et al. [**1**], that an alternative expression for n

$$n = \frac{\ln 4}{\ln\left(\frac{\sigma_{0.2}}{\sigma_{0.05}}\right)} \, , \qquad (3)$$

gives a more accurate description for the stress-strain behaviour for both austenitic and ferritic stainless steel grades.

In the present work, the accuracy of expressions (2) and (3) was evaluated by modelling a small number of randomly selected stress-strain curves using the parameters calculated with different expressions. The constant value of E_0 = *200 GPa* was used for the elastic modulus. The results showed that the accuracy of the Ramberg-Osgood stress-strain model is indeed greatly improved with the newly proposed expression (3) for n. An illustrative example is shown in Figure 15.

The n-values were also determined by VTT in work package 2 by means of an advanced nonlinear least squares (NLSQ) method [**2**]. Two different values, *200 GPa* and *220 GPa* were used for the initial elastic modulus E_0 in the fitting.

The n-values calculated based on 0.05% and 0.2% proof strength values and the ones obtained using the nonlinear optimization method are summarized in Table 9. The numbers are average values for three repeats.

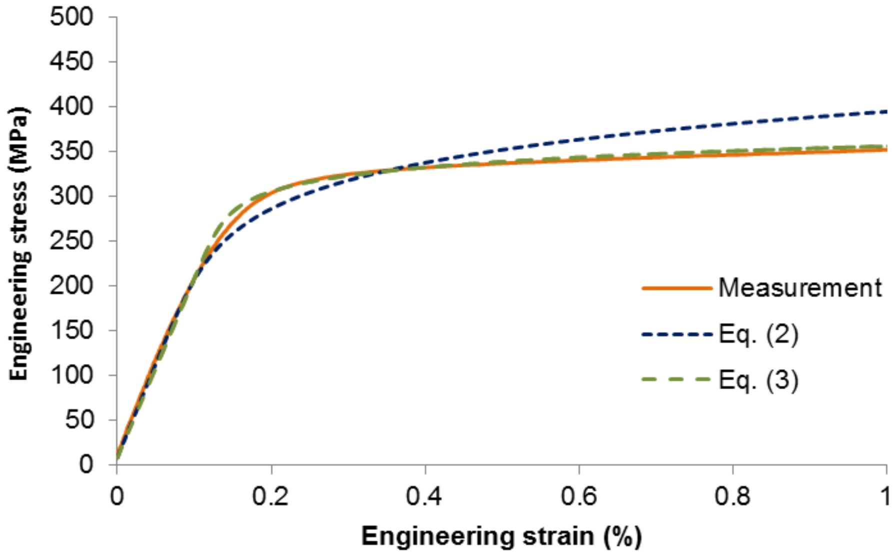

Figure 15. Stress-strain response measured for 4003-1 in the longitudinal direction. The dashed lines show the Ramberg-Osgood stress-strain model predictions with n-values calculated with different expressions.

Table 9. Summary of n-values determined using different methods.

		Equation (3)		NLSQ E_0 = 200 GPa		NLSQ E0 = 220 GPa	
Steel	Type	TD	RD	TD	RD	TD	RD
4003-1	CR	19.7	15.4	18.3	12.5	14.7	10.0
4016-1	CR	23.6	14.5	25.2	12.0	20.9	9.7
4016-2	CR	45.3	16.4	38.4	10.1	28.3	7.9
4016-3	HR	14.3	11.6	16.1	10.6	13.7	8.8
4509-3	HR	24.2	12.7	42.9	12.1	24.1	10.0
4509-1	CR	26.3	16.5	29.1	14.9	24.1	12.2
4509-2	CR	34.7	20.6	33.9	17.2	26.7	12.9
4521-1	CR	68.8	21.6	76.3	16.5	55.7	12.1
4521-2	CR	32.2	19.3	33.2	16.9	26.2	12.9
4621-1	CR	43.9	20.4	39.1	14.1	29.9	10.7

The *n*-values obtained using the nonlinear optimization method for different steels are shown in Figure 16. It can be seen that there is large dispersion in the *n*-values depending on direction, steel grade, steel producer and delivery condition. The scatter is particularly large in the transverse direction. The grouping of the points in the figure, however, suggests that the steels can be divided in two groups. The points corresponding to unstabilized grades 1.4003 and 1.4016 are located in a different part of the plot area than those corresponding to stabilized grades 1.4509, 1.4521 and 1.4621, as shown in Figure 17. The average *n*-values of both groups are given in Table 10. It is worth noting that the average *n*-values obtained in the present work are somewhat higher than the ones given in the EN 1993-1-3:2006 for the steel grades 1.4003 and 1.4016.

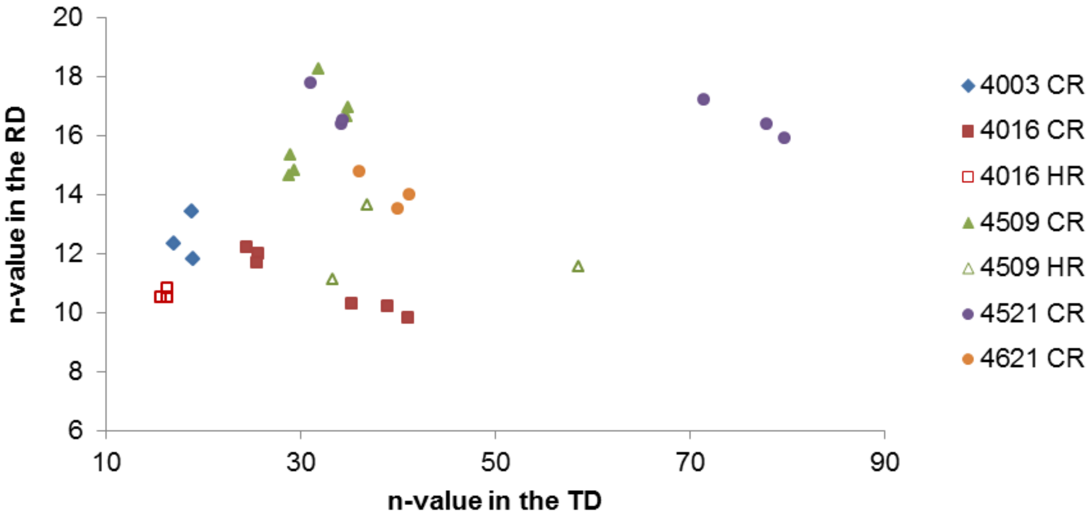

Figure 16. The *n*-values for cold-rolled (CR) and hot-rolled (HR) steels obtained using the nonlinear optimization method with $E_0 = 200\ GPa$.

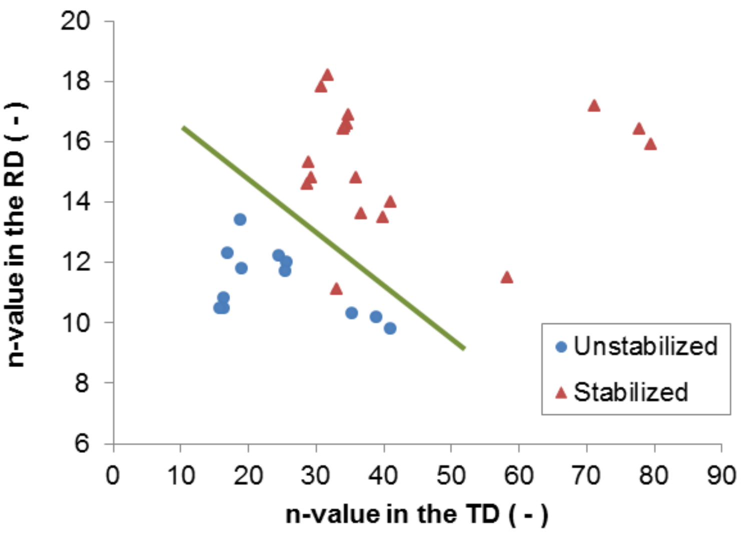

Figure 17. The *n*-values of unstabilized and stabilized grades obtained using the nonlinear optimization method with $E_0 = 200\ GPa$.

Table 10. Average *n*-values determined for the stabilized and unstabilized grades.

Group	Longitudinal			Transverse		
	n_3	n_{200}	n_{220}	n_3	n_{200}	n_{220}
Unstabilized grades	14	11	9	26	25	19
Stabilized grades	18	15	12	38	42	31

n_3 : *n*-value calculated with equation (3).
n_{200} : *n*-value obtained using the NLSQ method with $E_0 = 200\ GPa$.
n_{220} : *n*-value obtained using the NLSQ method with $E_0 = 220\ GPa$

6 Comparison of n-values determined using different methods

The coefficient *n* in the Ramberg-Osgood stress-strain model has been conventionally determined using equation (2). This expression has been successfully used for determining the *n*-values of different austenitic stainless steel and duplex grades in a number of studies. However, for the steels studied in the present work, this approach resulted in poor accuracy for the Ramberg-Osgood stress-strain model. Therefore, alternative methods were used for determining the coefficient *n*.

In order to analyse the *n*-values determined using different methods, a linear regression analysis was carried out on the results. The regression analysis revealed strong linear correlations between the *n*-values. The findings were confirmed by visual examination of the data.

There is a good linear correlation between the *n*-values calculated with equation (3) and those determined using the NLSQ optimization method with $E_0 = 200\ GPa$, Figure 18. On the average, the *n*-values calculated directly from the proof stress values were 4% lower than the optimal values determined using the NLSQ method with $E_0 = 200\ GPa$.

A comparison of *n*-values obtained with the NLSQ method using different elastic modulus values shows that changing the elastic modulus E_0 in the Ramberg-Osgood stress-strain model has an influence on the parameter *n*. If the elastic modulus used in the optimization was increased by 10%, the optimal *n*-value was decreased by 25%, Figure 19. The scatter in the *n*-values was also with the higher values of elastic modulus E_0.

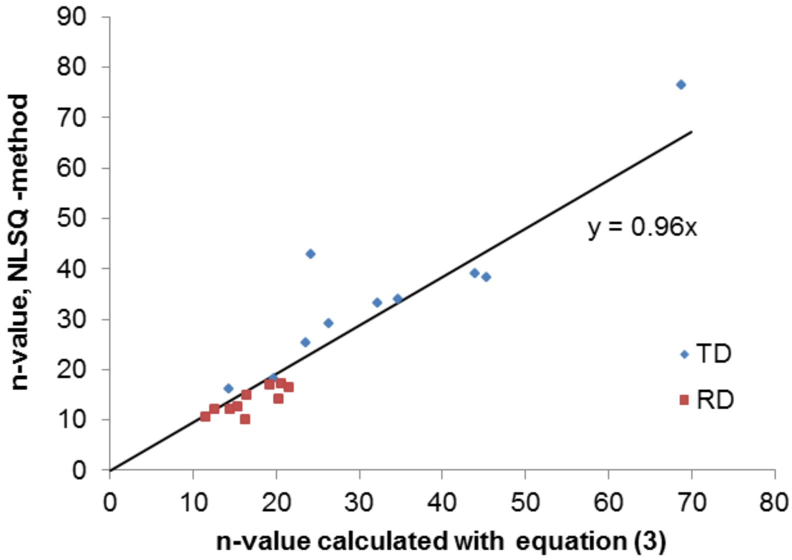

Figure 18. Correlation between the *n*-values calculated with equation (3) and n-values obtained with the NLSQ optimization method with $E_0 = 200\ GPa$.

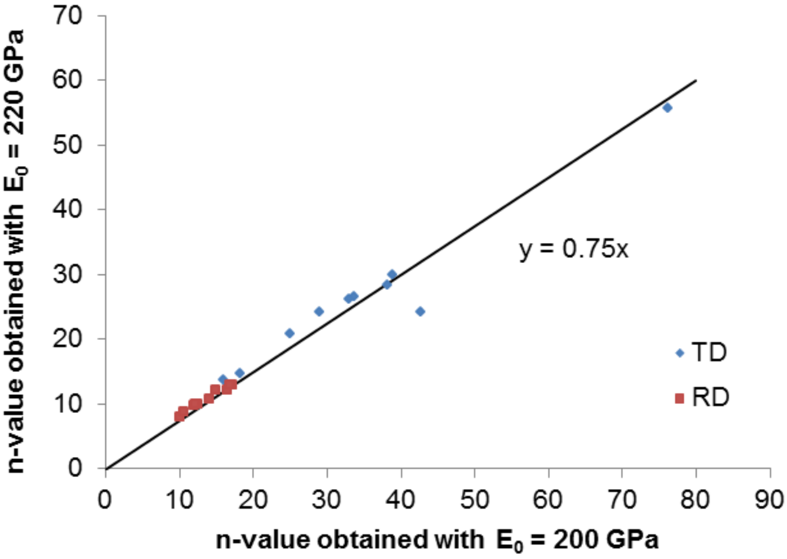

Figure 19. Correlation between *n*-values obtained using different values for the parameter E_0 in the Ramberg-Osgood stress-strain model.

Figure 20 demonstrates that there is also a strong linear correlation between the values calculated using equations (2) and (3). It is worth noting that the linear regression model between n_2 and n_3 crosses the line $n_2 = n_3$ at $n_2 \approx 6$. Therefore, the difference between n_2 and n_3 -values is negligible for small values of n. The n-values of austenitic and duplex grades are in the range from $n = 5$ to $n = 9$, i.e. in this region.

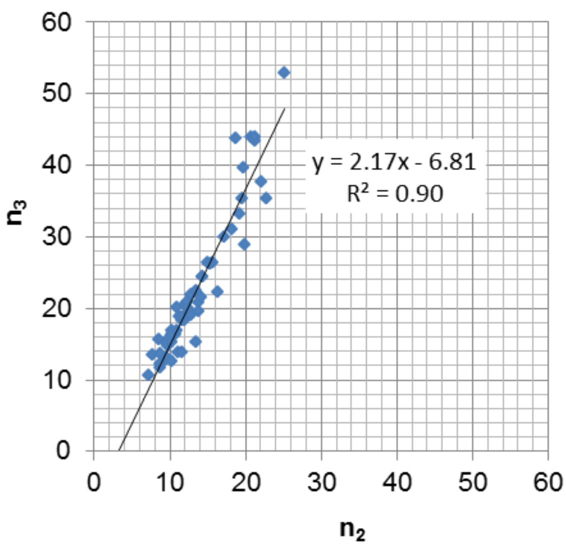

Figure 20. Correlation between *n*-values calculated using the equations (2) and (3). The subscript of *n* identifies the equation number.

The empirical correlations observed between the different values of coefficient n can be summarized as follows:

$$\begin{cases} n_3 = 2.17\, n_2 - 6.8 \\ n_{200} = 0.96\, n_3 \\ n_{220} = 0.75\, n_{200} \end{cases} \qquad (4)$$

where n_2 and n_3 are the values of coefficient n calculated with equations (2) and (3), respectively, and n_{200} and n_{220} are the values obtained with the nonlinear least squares optimization method using different values for E_0.

The results of the comparison can be summarized as follows:

- The optimal n-value determined using the nonlinear optimization method depends on the value of the initial elastic modulus E_0 used in the Ramberg-Osgood stress-strain model. If the elastic modulus E_0 was increased by 10%, the n-value decreased by 25%. It follows that the coefficients n and E_0 should be provided together in the design guidance.
- The values of coefficient n calculated with the equation (3) were close to the ones obtained using the NLSQ optimization method with $E_0 = 200\ GPa$.
- For small values of $n < 10$, the differences between the n-values determined using different methods diminish.

7 Summary and Conclusions

- Tension and compression tests were carried out to characterize the stress-strain behaviour of commercial ferritic stainless steel grades 1.4003, 1.4016, 1.4509, 1.4521 and 1.4621. The material properties were determined for virgin sheets supplied by three European steel producers. The tests were carried out on samples orientated in the longitudinal and transverse directions.

- All studied steels had significant overstrength and excess ductility with respect to the minimum requirements specified in the material standard prEN 10088-2:2005. On the average, the overstrength was 40% of the minimum value specified by the standard.

- All studied steels had sufficient work-hardening capacity and ductility for application in load-bearing structural members. The average tensile strength to 0.2% proof strength ratio was 1.34 and 1.40 in the transverse and longitudinal directions, respectively. The average elongation at fracture was A5 = 43%.

- The studied steels did not exhibit tension-compression anisotropy. The difference between the 0.2% proof strength values measured in tension and in compression was smaller than the experimental uncertainly of the 0.2% proof strength.

- The 0.2% proof strength was on the average 12% higher in the transverse direction than in the longitudinal direction. The transverse-longitudinal anisotropy was similar in tension and in compression.

- The coefficient n defining the non-linearity of the stress-strain curve is conventionally determined by means of an analytic expression using the Rp0.01 and Rp0.2 values measured in tensile test. This method gave poor accuracy in the present work. An improved accuracy was obtained using an alternative expression based on the Rp0.05 and Rp0.2 values.

- The n-values were also determined by VTT by means of an advanced nonlinear least squares optimization method [**2**]. Two different values were used for the elastic modulus E_0. The results show, that the value of n depends on the elastic modulus E_0 in the Ramberg-Osgood stress-strain model. If the elastic modulus E_0 was increased by 10%, the n-value decreased by 25%. It follows that the coefficients n and E_0 should be provided together in the design guidance.

- There was significant dispersion in the n-values depending on direction, steel grade, steel producer and delivery condition. The scatter was particularly large in the transverse direction.

- Closer analysis of the experimental n-values suggests that the investigated ferritic stainless steels grades can be divided in two groups with similar characteristics in each group. The first group contains the unstabilized grades 1.4003 and 1.4016, and the second group contains the stabilized grades 1.4509, 1.4521 and 1.4621. Average n-values were calculated for both groups of steels. The average n-values obtained in this work were somewhat higher than the ones given in the EN 1993-1-3:2006 for the steel grades 1.4003 and 1.4016.

References

1 Real, E., Arrayago, I., Mirambell, E. and Westeel, R. Comparative study of analytical expressions for the modelling of stainless steel behaviour. *Thin-Walled Structures* (Accepted for publication).

2 Hradil, P. *SAFSS Deliverable WP2, Task 2.4 : Optimisation of stainless steel*. VTT - Technical Research Centre of Finland, Espoo, Finland, 2013.

Appendices

A. Tension test stress-strain curves

B. Tension test results

C. Compression test results

D. Values of parameter *n*

Stress-strain curves for all tested steels

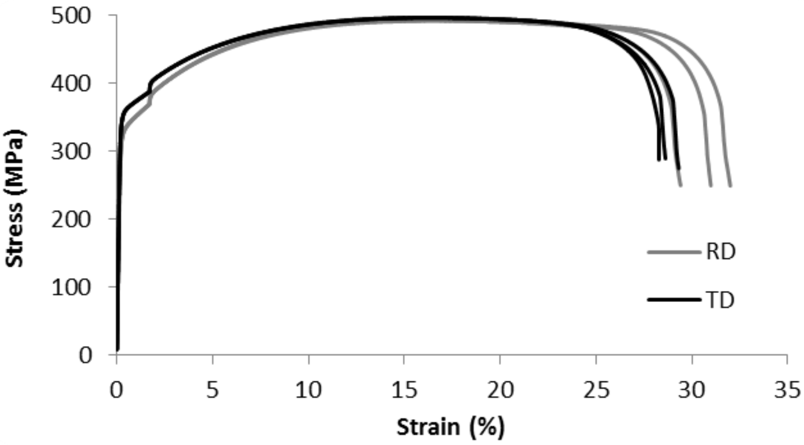

4003-1

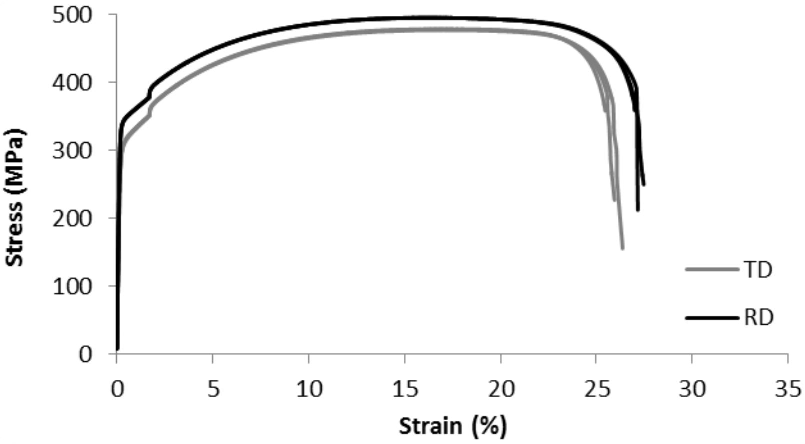

4016-1

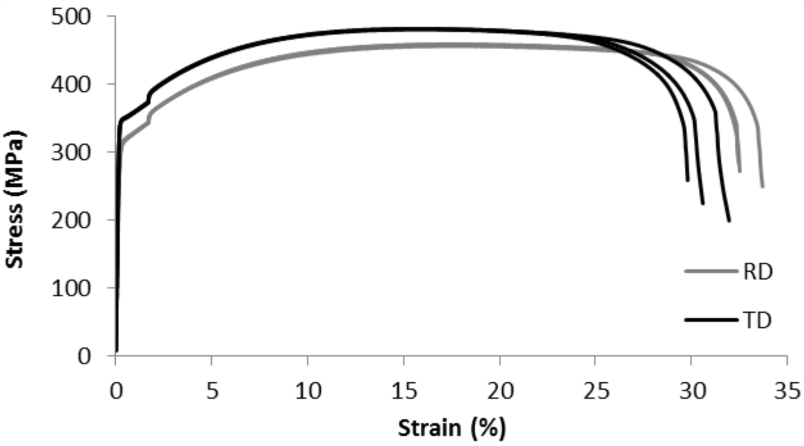

4016-2

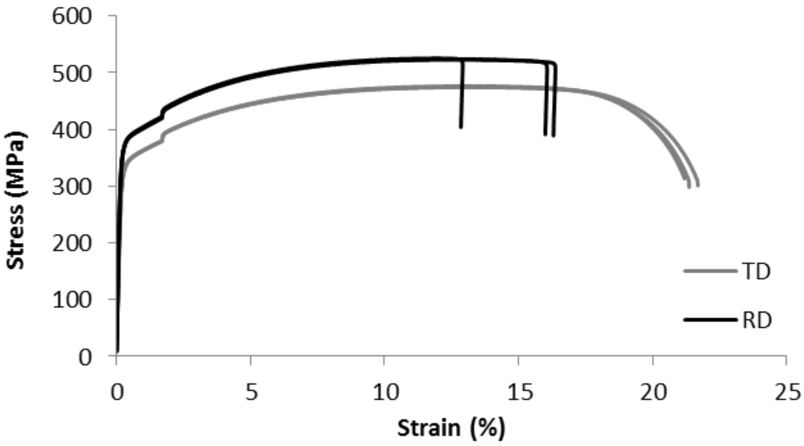

4016-3

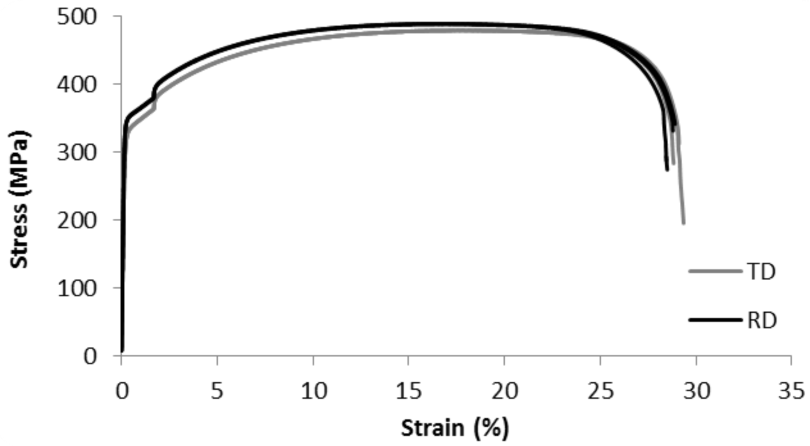

4509-1

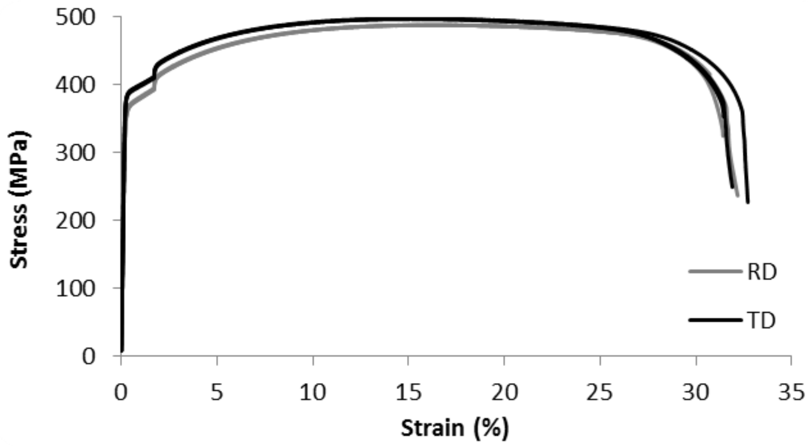

4509-2

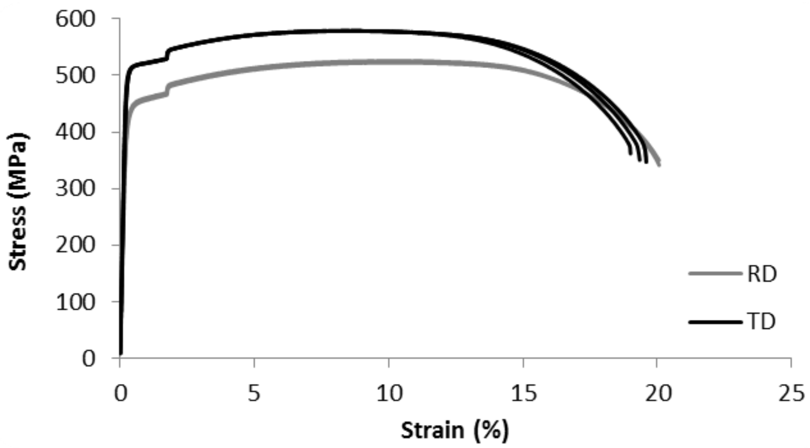

4509-3

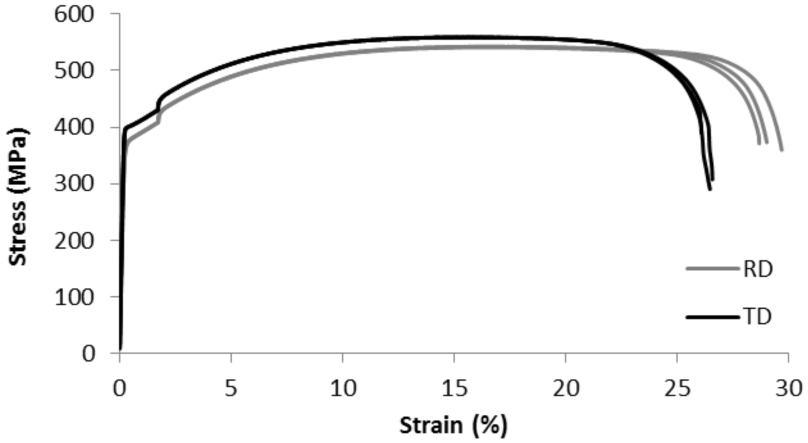

4521-1

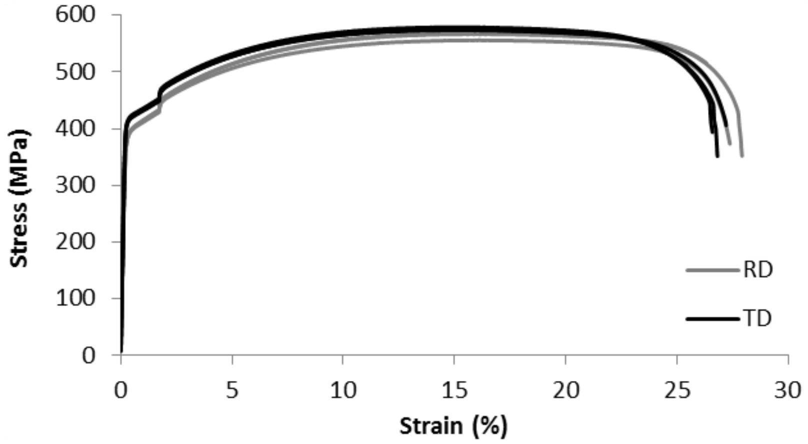

4521-2

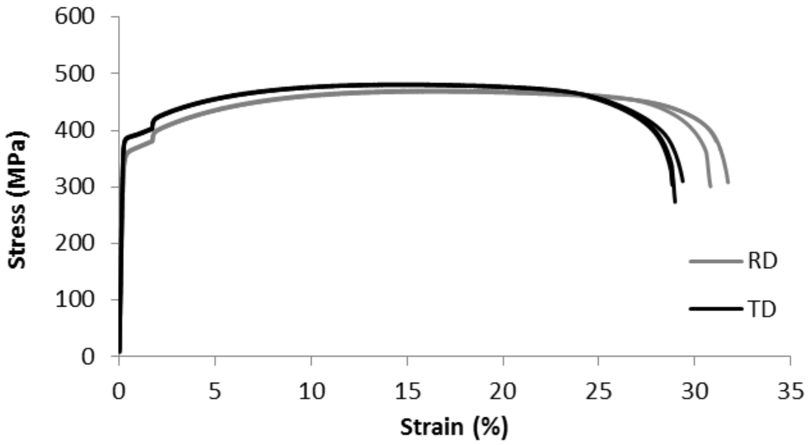

4621-1

Summary of Tension Test Results

Table 1. Tension test results for all studied steels.

Nr	Steel	Direction	E (GPa)	Rp 0,01 (N/mm²)	Rp 0,05 (N/mm²)	Rp 0,1 (N/mm²)	Rp 0,2 (N/mm²)	Rp 1,0 (N/mm²)	Rm (N/mm²)	Ag (%)	A* (%)	A5 (%)
1	4003-1	TD	199	287	334	348	357	378	497	15.8	28	44
2	4003-1	TD	203	276	331	346	357	378	496	16.2	30	47
3	4003-1	TD	204	282	332	346	357	377	497	16.1	29	46
4	4003-1	RD	209	224	297	316	329	356	493	15.8	30	48
5	4003-1	RD	184	246	304	319	330	357	494	16.2	33	54
6	4003-1	RD	189	233	303	318	331	357	492	16.5	31	50
7	4016-1	TD	221	272	323	336	344	366	496	16.1	27	42
8	4016-1	TD	216	279	325	336	344	366	496	16.1	27	40
9	4016-1	TD	217	280	326	337	345	367	496	15.7	29	45
10	4016-1	RD	195	220	281	299	311	339	479	16.7	25	36
11	4016-1	RD	190	230	284	300	312	339	477	17.1	26	38
12	4016-1	RD	186	226	282	298	309	337	478	16.7	27	40
13	4016-2	TD	207	304	339	346	350	364	482	15.8	32	51
14	4016-2	TD	201	300	337	345	349	364	482	15.4	33	55
15	4016-2	TD	196	309	339	345	348	363	481	15.7	30	48
16	4016-2	RD	177	233	290	308	317	334	456	17.1	35	56
17	4016-2	RD	172	245	292	306	315	333	459	17.5	33	53
18	4016-2	RD	177	234	286	302	313	333	459	17.5	32	51
19	4016-3	TD	214	303	346	365	379	407	523	12.1	(16)	(18)
20	4016-3	TD	223	289	343	363	379	408	524	12.1	(16)	(18)
21	4016-3	TD	229	293	344	364	380	409	525	11.9	(13)	(13)
22	4016-3	RD	195	241	301	323	339	368	476	13.0	21	25
23	4016-3	RD	206	223	297	321	338	367	474	12.8	22	26
24	4016-3	RD	195	242	302	322	338	367	475	13.0	21	25
25	4509-1	TD	222	290	333	344	351	369	489	16.2	29	44
26	4509-1	TD	222	288	334	344	352	370	490	16.4	29	44
27	4509-1	TD	220	288	332	343	350	368	489	16.6	29	45
28	4509-1	RD	199	252	305	321	331	353	479	18.0	29	43
29	4509-1	RD	204	251	304	321	331	352	479	17.4	29	43
30	4509-1	RD	201	247	304	320	331	353	479	17.3	29	43
31	4509-2	TD	206	342	375	384	390	404	498	15.2	33	55
32	4509-2	TD	208	330	372	382	389	403	497	14.8	33	57
33	4509-2	TD	206	338	373	381	387	401	497	14.8	33	56
34	4509-2	RD	197	280	340	356	366	383	488	15.9	31	50
35	4509-2	RD	194	294	345	358	367	384	488	16.1	34	56
36	4509-2	RD	196	288	345	359	369	386	488	15.8	34	57
37	4509-3	TD	227	426	481	500	512	524	579	8.3	20	24
38	4509-3	TD	226	415	481	502	513	525	579	7.9	19	24

39	4509-3	TD	241	441	489	504	513	524	578	8.1	20	24
40	4509-3	RD	218	314	395	422	442	463	526	9.6	21	25
41	4509-3	RD	194	320	394	418	438	460	522	9.7	21	25
42	4509-3	RD	201	329	395	421	441	463	525	9.7	21	25
43	4521-1	TD	213	354	393	399	401	418	559	15.4	27	42
44	4521-1	TD	206	360	393	399	401	418	559	15.4	26	39
45	4521-1	TD	211	358	393	398	401	417	559	15.1	30	47
46	4521-1	RD	192	289	351	366	375	396	541	16.1	29	44
47	4521-1	RD	195	287	352	368	376	396	542	16.2	29	44
48	4521-1	RD	188	296	353	367	375	396	543	16.2	30	46
49	4521-2	TD	211	356	399	409	416	437	574	14.7	29	46
50	4521-2	TD	214	353	401	412	420	441	579	14.8	29	46
51	4521-2	TD	213	358	401	410	417	438	574	14.8	27	42
52	4521-2	RD	196	303	364	381	392	417	556	15.7	27	42
53	4521-2	RD	194	318	368	384	395	421	567	15.8	28	44
54	4521-2	RD	196	305	366	382	394	420	568	15.4	28	45
55	4621-1	TD	207	328	373	381	385	395	480	14.8	29	52
56	4621-1	TD	200	334	374	382	386	396	481	14.7	32	58
57	4621-1	TD	207	336	375	383	387	397	482	14.2	29	53
58	4621-1	RD	181	281	336	350	359	373	469	16.2	32	56
59	4621-1	RD	188	274	336	352	360	374	470	15.7	32	56
60	4621-1	RD	183	282	335	350	359	373	468	15.9	32	56

* = A80 for cold-rolled and A50 for hot-rolled strip.
( ) = Fracture occurred near the specimen shoulder, ultimate tensile strain could not be determined accurately.

Table 1. Compression test results for all studied steels.

Nr	Steel	Direction	E (GPa)	Rp0,01 (N/mm²)	Rp0,1 (N/mm²)	Rp0,2 (N/mm²)	Rp1,0 (N/mm²)
1	4003-1	TD	221	282	356	366	395
2	4003-1	TD	238	275	343	354	383
3	4003-1	TD	238	280	355	366	395
4	4003-1	RD	221	206	294	315	362
5	4003-1	RD	185	204	282	303	351
6	4003-1	RD	208	209	293	313	359
7	4016-1	TD	208	268	327	337	373
8	4016-1	TD	208	258	332	343	377
9	4016-1	TD	238	274	338	350	388
10	4016-1	RD	194	204	282	302	346
11	4016-1	RD	183	197	284	304	344
12	4016-1	RD	175	201	276	294	337
13	4016-2	TD	217	264	342	353	381
14	4016-2	TD	227	262	343	351	375
15	4016-2	TD	201	273	341	348	373
16	4016-2	RD	185	209	292	310	343
17	4016-2	RD	185	210	291	309	344
18	4016-2	RD	187	222	298	314	347
19	4016-3	TD	250	296	388	401	435
20	4016-3	TD	228	342	390	399	431
21	4016-3	TD	217	253	380	393	426
22	4016-3	TD	250	296	388	401	435
23	4016-3	TD	228	342	390	399	431
24	4016-3	TD	217	253	380	393	426
25	4016-3	RD	202	222	321	337	374
26	4016-3	RD	203	217	314	332	369
27	4016-3	RD	213	215	315	332	369
28	4509-1	TD	215	268	343	353	383
29	4509-1	TD	212	277	344	353	380
30	4509-1	TD	222	238	333	349	379
31	4509-1	RD	208	187	297	322	360
32	4509-1	RD	204	199	298	321	362
33	4509-2	TD	200	312	382	392	417
34	4509-2	TD	242	294	376	388	416
35	4509-2	TD	223	293	379	388	413
36	4509-2	RD	195	227	344	363	398
37	4509-2	RD	218	227	342	362	400
38	4509-2	RD	208	249	339	357	392

39	4509-3	TD	243	348	490	508	534
40	4509-3	TD	250	370	493	511	533
41	4509-3	TD	223	350	492	512	538
42	4509-3	RD	200	291	416	443	480
43	4509-3	RD	217	300	417	445	484
44	4509-3	RD	217	217	405	438	479
45	4521-1	TD	296	277	395	409	436
46	4521-1	TD	299	246	396	406	429
47	4521-1	RD	209	251	367	386	412
48	4521-1	RD	214	255	367	386	412
49	4521-1	RD	217	221	364	387	434
50	4521-2	TD	231	350	421	431	464
51	4521-2	TD	227	315	415	428	461
52	4521-2	TD	257	333	416	428	460
53	4521-2	RD	225	248	364	386	433
54	4521-2	RD	217	227	361	386	433
55	4521-2	RD	208	247	338	353	380
56	4621-1	TD	239	304	367	374	393
57	4621-1	TD	315	228	373	387	405
58	4621-1	RD	197	223	327	342	368
59	4621-1	RD	208	247	338	353	380

Summary of n-values obtained using the optimization method.

This appendix summarizes the values of coefficient n in the Ramberg-Osgood stress-strain model calculated obtained with different methods.

Table 1. Values of parameter n obtained using different methods for all tests.

Nr	Steel	Direction	Rp 0,01 (N/mm²)	Rp 0,05 (N/mm²)	Rp 0,2 (N/mm²)	n_2 (-)	n_3 (-)	n_{200} (-)	n_{220} (-)
1	4003-1	TD	287	334	357	13.7	20.8	18.9	15.2
2	4003-1	TD	276	331	357	11.6	18.3	17.0	13.7
3	4003-1	TD	282	332	357	12.7	19.1	19.0	15.3
4	4003-1	RD	224	297	329	7.8	13.5	13.4	10.8
5	4003-1	RD	246	304	330	10.2	16.9	12.3	9.8
6	4003-1	RD	233	303	331	8.5	15.7	11.8	9.3
7	4016-1	TD	272	323	344	12.8	22.0	24.5	20.2
8	4016-1	TD	279	325	344	14.3	24.4	25.7	21.4
9	4016-1	TD	280	326	345	14.4	24.5	25.5	21.1
10	4016-1	RD	220	281	311	8.7	13.7	12.2	10.0
11	4016-1	RD	230	284	312	9.8	14.7	12.0	9.7
12	4016-1	RD	226	282	309	9.6	15.2	11.7	9.5
13	4016-2	TD	304	339	350	21.3	43.4	41.0	29.9
14	4016-2	TD	300	337	349	19.8	39.6	35.3	27.4
15	4016-2	TD	309	339	348	25.2	52.9	38.9	27.6
16	4016-2	RD	233	290	317	9.7	15.6	9.8	7.5
17	4016-2	RD	245	292	315	11.9	18.3	10.3	8.3
18	4016-2	RD	234	286	313	10.3	15.4	10.2	8.0
19	4016-3	TD	303	346	379	13.4	15.2	16.3	13.8
20	4016-3	TD	289	343	379	11.0	13.9	15.7	13.3
21	4016-3	TD	293	344	380	11.5	13.9	16.3	13.9
22	4016-3	RD	241	301	339	8.8	11.7	10.5	8.7
23	4016-3	RD	223	297	338	7.2	10.7	10.5	8.8
24	4016-3	RD	242	302	338	9.0	12.3	10.8	8.9
25	4509-1	TD	290	333	351	15.7	26.3	29.4	24.3
26	4509-1	TD	288	334	352	14.9	26.4	29.0	23.8
27	4509-1	TD	288	332	350	15.4	26.3	28.8	24.3
28	4509-1	RD	252	305	331	11.0	16.9	14.8	12.2
29	4509-1	RD	251	304	331	10.8	16.3	15.3	12.4
30	4509-1	RD	247	304	331	10.2	16.3	14.6	11.9
31	4509-2	TD	342	375	390	22.8	35.3	34.9	28.2
32	4509-2	TD	330	372	389	18.2	31.0	31.9	24.6
33	4509-2	TD	338	373	387	22.1	37.6	34.8	27.2
34	4509-2	RD	280	340	366	11.2	18.8	16.9	12.7
35	4509-2	RD	294	345	367	13.5	22.4	18.2	13.4
36	4509-2	RD	288	345	369	12.1	20.6	16.6	12.7
37	4509-3	TD	426	481	512	16.3	22.2	36.8	20.9

38	4509-3	TD	415	481	513	14.1	21.5	33.3	20.0
39	4509-3	TD	441	489	513	19.8	28.9	58.5	31.5
40	4509-3	RD	314	395	442	8.8	12.3	13.6	11.2
41	4509-3	RD	320	394	438	9.5	13.1	11.1	9.0
42	4509-3	RD	329	395	441	10.2	12.6	11.5	9.9
43	4521-1	TD	354	393	401	24.0	68.8	77.9	58.6
44	4521-1	TD	360	393	401	27.8	68.8	71.4	49.3
45	4521-1	TD	358	393	401	26.4	68.8	79.7	59.2
46	4521-1	RD	289	351	375	11.5	21.0	16.4	12.0
47	4521-1	RD	287	352	376	11.1	21.0	17.2	12.8
48	4521-1	RD	296	353	375	12.7	22.9	15.9	11.5
49	4521-2	TD	356	399	416	19.2	33.2	34.2	26.8
50	4521-2	TD	353	401	420	17.2	29.9	31.0	24.6
51	4521-2	TD	358	401	417	19.6	35.4	34.3	27.3
52	4521-2	RD	303	364	392	11.6	18.7	16.4	12.4
53	4521-2	RD	318	368	395	13.8	19.6	17.8	13.4
54	4521-2	RD	305	366	394	11.7	18.8	16.5	12.9
55	4621-1	TD	328	373	385	18.7	43.8	40.0	31.3
56	4621-1	TD	334	374	386	20.7	43.9	36.1	27.4
57	4621-1	TD	336	375	387	21.2	44.0	41.2	31.0
58	4621-1	RD	281	336	359	12.2	20.9	13.5	10.2
59	4621-1	RD	274	336	360	11.0	20.1	14.8	11.3
60	4621-1	RD	282	335	359	12.4	20.0	14.0	10.6

n_2 = parameter *n* calculated with equation (2).
n_3 = parameter *n* calculated with equation (3).
n_{200} = parameter *n* obtained using the optimization method with E_0 = *200 GPa.*
n_{220} = parameter *n* obtained using the optimization method with E_0 = *220 GPa.*